TECHNISCHE UNIVERSITÄT BERLIN

Distributed Control of Linearized Navier-Stokes Equations via Discretized Input/Output Maps

Jan Heiland   Volker Mehrmann

Preprint 2011/12

Abstract

The construction of reduced order models for flow control via a direct discretization of the input/output behavior of the system is discussed. The spatially discretized equations are linearized such that an explicit formula for the corresponding input/output map can be used to generate a matrix representation of the input/output map. Estimates for the approximation error are derived and the applicability is illustrated via a numerical example for the control of a driven cavity flow.

1   Introduction

In the research on flow control recently many promising results are obtained [33, 34]. Many of these results are based on experimental setups, whereas the model based solution of flow control problems is still at an early stage. Up to now, still best practice heuristic methods have a practical advantage compared to mathematical approaches with guaranteed robustness and convergence rates. This is mainly due to the fact that the simulation and optimization of flows leads to very large nonlinear models, while numerical control algorithms perform already very efficiently on linear models of moderate size [46, 4].

To overcome this discrepancy one can use reduced order models that still capture the essential dynamics, c.f. [1, 5]. These lower order approximations can be obtained using physical insight [37, 39, 40] and/or mathematical techniques [1, 7, 38].

This paper proposes a model reduction method that focusses on the input/output behavior rather than on the state dynamics. We consider the so called *input/output (I/O) map* that describes a physical system equipped with actuators and sensors in terms of the relation between an actuation (input) and the related output, c.f. Figure 1.

The approach that is presented here can be interpreted as a model identification algorithm, c.f. [43], and is well suited for black-box identification [3, 29] in simulations and experiments. Other approaches to an approximation of the I/O map are balanced truncation [20], moment matching [16] and proper orthogonal decomposition [42]. In particular, balanced truncation has been investigated for spatially discretized linearized Navier-Stokes equations (LNSE), see [28, 45]. This strategy is motivated by the observation that control often acts locally in time, and therefore the design of a controller based on an approximated linear model still promises a good result.

To model the distributed control, the volume force in the Navier-Stokes equation is extended by a control term that acts in a small region of the domain. The publications [8, 11, 21, 22, 23, 24, 28, 31, 30, 32] represent a small selection of contributions to the optimal control of Navier-Stokes equations. Results using linearized equations to set up control
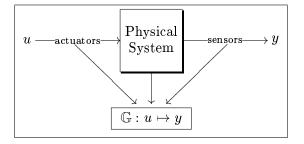

Figure 1: Schematic illustration of the I/O map for a physical system.

schemes can be found in [41, 8, 15]. At this stage the extension of this approach to the case that the flow is controlled via a source acting only at the boundary, i.e., via the boundary conditions in the partial differential equation model, is much less established, see, e.g., [24, 31, 32].

Our new approach is based on a recently introduced general semigroup approach [27, 43] for linear time invariant (LTI) systems of abstract ordinary differential equations. Here, we will extend this approach to abstract differential-algebraic systems and with this the applicability to flow control problems.

Consider model problems governed by the non-dimensional Navier-Stokes equation (NSE), extended by terms accounting for the input and output,

$$V_t + (V \cdot \nabla)V + \nabla P - \frac{1}{Re}\triangle V = f + \mathcal{B}u, \tag{1a}$$

$$\nabla \cdot V = 0, \tag{1b}$$

$$y = \mathcal{C}V, \tag{1c}$$

together with appropriate initial and boundary conditions. These equations describe the relation between an input u and an output y, with respect to the evolution of the fluid velocity V and the pressure P for a time interval in a spatial domain.

A linearization of (1) along a reference velocity V_∞ leads to the linearized Navier-Stokes equations (LNSE)

$$V_t + (V_\infty \cdot \nabla)V + (V \cdot \nabla)V_\infty + \nabla P - \frac{1}{Re}\triangle V = (V_\infty \cdot \nabla)V_\infty + f + \mathcal{B}u, \tag{2a}$$

$$\nabla \cdot V = 0, \tag{2b}$$

$$y = \mathcal{C}V. \tag{2c}$$

This linear model, together with discrete input and output spaces, enables the construction of a finite dimensional discrete linear I/O-operator.

In this paper we discuss both general and particular aspects of the use of I/O maps in flow control problems. Section 2 introduces the notion of an abstract optimal control problem and points out the advantages of I/O maps in this setup. Section 3 explains how the I/O map may be discretized and how a matrix representation is obtained. Section 4 introduces a mathematical framework for differential-algebraic equations and establishes the I/O map for the spatially discretized linearized NSE in an explicit form. As the central analytical result, Theorem 4.2 formulates the necessary conditions on the regularity of the inputs. In addition Lemma 4.2 quantifies these conditions for a wide class of common finite element discretizations of the Navier-Stokes equations. The error analysis for the discrete I/O map is derived in Section 5 and addresses mainly the I/O approximation error. The application of this approach to the control of the flow in a driven cavity is demonstrated by a numerical example in Section 6, studying the model for the I/O map, the discretization of the input and output spaces and an experimental error analysis. The optimal control of such a flow is illustrated by an numerical example in Section 7. Section 8 completes this work with summarizing conclusions and an outlook on future research.

2   I/O Maps in PDE Constrained Control

The optimal control of Navier-Stokes equations (NSE) via the input/output map is a special case of PDE constraint optimal control and fits into the general framework of abstract

optimization problems as defined e.g. in [21].

For the abstract formulation, the control variables and design parameters are typically combined in the variable u, the output variables are denoted by y, and functions $F(y, u)$ and $\mathcal{J}(y, u)$ define the constraints and the cost functional, respectively. Then the control problem is to determine controls u that give outputs y such that

$$\mathcal{J}(y, u) \to \min \tag{3a}$$

subject to

$$F(y, u) = 0. \tag{3b}$$

If the constraints F are given by a system of partial differential equations (PDE), describing for example the actuators, the behavior of the system and the sensors, the problem as given in (3) is called *PDE constrained optimization*.

A conventional approach for the control of unsteady PDE systems is to approximate it by a system of ordinary differential equations, derived from a spatial discretization. Here, however, we focus directly on the I/O behavior of the original system. The construction of a discretized I/O map leads to an effective treatment of the control problem in several respects.

Firstly, if the system is represented by an I/O operator $\mathbb{G}$ that maps the control u onto the output $y = \mathbb{G}u$, then the formulation of a PDE constraint optimal control problem as given in (3) simplifies. Since $\mathbb{G}$ also implicitly contains the constraints, the optimal control problem described above turns into an unconstrained minimization problem:

Determine controls u such that

$$\mathcal{J}(\mathbb{G}u, u) \to \min .$$

In general, however, the computation of $\mathbb{G}u$ during an optimization still requires an extremely large computational effort, since every evaluation of the map requires a forward solve of the non-stationary NSE, so that an appropriate model reduction is important. For this model reduction we propose to use a discretization of the I/O map and not of the forward system. In the case of a linear PDE this leads to a matrix representation of the I/O map as suggested in [43]. Then the computation of the system response for a given input reduces to a matrix vector multiplication. In addition, for the application in control design and optimization the use of discrete I/O maps is well suited for error estimation, adaptivity and practical relevance.

Secondly, the error estimates for an I/O map as given in Section 5.1 are focused on the relevant system response, whereas error bounds for the internal state variables often provide only rough estimates for the error in the I/O behavior. The I/O map discretization allows the easy use of goal oriented error estimation as has been shown in [43, Ch. 4].

Third, the use of hierarchical bases for the input and the output enables a straight-forward enrichment or reduction of the model. Furthermore, a *singular value decomposition* of the finite dimensional I/O map directly identifies the relevant input and output functions, which can be used for an efficient system specific formulation, see again [43].

Finally, in practical applications of flow control, the actuation often uses a finite set of inputs, as, e.g. various sine functions. Also the sensors measuring the output often deliver discrete representations of the signal.

3 Discrete I/O Mapping

The presented framework applies to linear time invariant (LTI) systems, that can be written as an abstract differential-algebraic system

$$E\dot{z}(t) + Az(t) = f(t) + Bu(t), \quad t \in (0, T] \tag{4a}$$

$$z(0) = z_0, \tag{4b}$$

$$y(t) = Cz(t). \tag{4c}$$

For fixed $t \in [0, T]$ the state variable z is supposed to belong to a Hilbert space Z, e.g. $Z = L_2(\Omega)$ on a domain $\Omega \subset \mathbb{R}^{d_\Omega}$, and the control $u(t)$ and output $y(t)$ are assumed to be in Hilbert spaces describing the signal states, as e.g. $U = L_2(\Sigma)$ and $Y = L_2(\Theta)$, respectively, with domains $\Sigma \subset \mathbb{R}^{d_\Sigma}$ and $\Theta \subset \mathbb{R}^{d_\Theta}$.

Furthermore, let $B : U \mapsto Z$ and $C : Z \mapsto Y$ be bounded linear operators. This allows the treatment of problems with distributed control and observation, c.f. [6, 36, 43]. Provided that the linear operators E, A are given in such a way, that for given z_0, u the system (4) has a unique solution, c.f. [47], it implicitly defines a mapping

$$\mathbb{G} : \mathcal{U} \to \mathcal{Y}, u \mapsto y,$$

that associates an input u with the respective solution y of system (4), for inputs and outputs from spaces

$$\mathcal{U} := L_2([0, T]; U) \quad \text{and} \quad \mathcal{Y} := L_2([0, T]; Y).$$

Throughout this paper $\mathbb{G}$ is assumed to be linear and bounded, in a general context these properties depend on the underlying system and have to be investigated.

For the analysis of the numerical methods and for the implementation, the spatial and temporal discretization of the input $u \in \mathcal{U}$ and output $y \in \mathcal{Y}$ signals has to be discussed in detail. Consider the four families $\{U_{h_1}\}_{h_1 > 0}$, $\{Y_{h_2}\}_{h_2 > 0}$, $\{\mathcal{R}_{k_1}\}_{k_1 > 0}$ and $\{\mathcal{S}_{k_2}\}_{k_2 > 0}$ of subspaces

$$U_{h_1} \subset U, \quad Y_{h_2} \subset Y, \quad \mathcal{R}_{k_1} \subset L_2([0, T]), \quad \mathcal{S}_{k_2} \subset L_2([0, T]),$$

of finite dimensions $p(h_1) = \dim U_{h_1}$, $q(h_2) = \dim Y_{h_2}$, $r(k_1) = \dim \mathcal{R}_{k_1}$, $s(k_2) = \dim \mathcal{S}_{k_2}$. Using a tensor product representation, we approximate the input and output signals by representatives in subspaces $\mathcal{U}_{h_1 k_1} \subset \mathcal{U}$ and $\mathcal{Y}_{h_2 k_2} \subset \mathcal{Y}$ of finite dimensions d_U and d_Y, defined via

$$\mathcal{U}_{h_1 k_1} = \{u \in \mathcal{U} : u(t, \cdot) \in U_{h_1}, u(\cdot, \sigma) \in \mathcal{R}_{k_1} \text{ for almost every } t \in [0, T], \sigma \in \Sigma\},$$

$$\mathcal{Y}_{h_2 k_2} = \{y \in \mathcal{Y} : y(t, \cdot) \in Y_{h_2}, y(\cdot, \theta) \in \mathcal{S}_{k_2} \text{ for almost every } t \in [0, T], \theta \in \Theta\},$$

respectively, where $\Sigma \subset \mathbb{R}^{d_\Sigma}$ and $\Theta \subset \mathbb{R}^{d_\Theta}$ denote the domains of control and observation. We then consider the finite dimensional map

$$\mathbb{G}_S := \mathscr{P}_{\mathcal{Y}, h_2 k_2} \mathbb{G} \mathscr{P}_{\mathcal{U}, h_1 k_1},$$

where $\mathscr{P}_{\mathcal{U}, h_1 k_1}$ and $\mathscr{P}_{\mathcal{Y}, h_2 k_2}$ denote the orthogonal projectors onto the respective finite dimensional subspaces. To obtain a matrix representation, four families of bases $\{\mu_1, \ldots, \mu_p\}$ of U_{h_1}, $\{\nu_1, \ldots, \nu_q\}$ of Y_{h_2}, $\{\phi_1, \ldots, \phi_s\}$ of $\mathcal{S}_{k_1}$ and $\{\psi_1, \ldots, \psi_r\}$ of $\mathcal{R}_{k_2}$ with their corresponding mass matrices

$$M_{U, h_1} = [(\mu_i, \mu_j)_U]_{i, j = 1, \ldots, p}$$

and analogously defined M_{Y,h_2}, $M_{\mathcal{R},k_1}$ and $M_{\mathcal{S},k_2}$, are introduced. Then the discrete signals $u \in \mathcal{U}_{h_1 k_1}$ and $y \in \mathcal{Y}_{h_2 k_2}$ can be represented by means of the tensor product bases

$$u(t,\sigma) = \sum_{k=1}^{p}\sum_{i=1}^{r} \mathbf{u}_i^k \phi_i(t)\mu_k(\sigma) \quad \text{and} \quad y(t,\theta) = \sum_{l=1}^{q}\sum_{j=1}^{s} \mathbf{y}_j^l \psi_j(t)\nu_l(\theta), \tag{5}$$

where $\mathbf{u}_i^k$ are the elements of a block-structured vector $\mathbf{u} \in \mathbb{R}^{pr}$ containing p blocks of length r and $\mathbf{y} \in \mathbb{R}^{qs}$ is defined similarly.

The mass matrices of the tensor product bases used in (5) have the form

$$M_{\mathcal{U},h_1 k_1} = M_{U,h_1} \otimes M_{\mathcal{R},k_1} \in \mathbb{R}^{pr \times pr} \quad \text{and} \quad M_{\mathcal{Y},h_2 k_2} = M_{Y,h_2} \otimes M_{\mathcal{S},k_2} \in \mathbb{R}^{qs \times qs}.$$

They are positive definite and define, for instance via

$$(\mathbf{v},\mathbf{w})_{\mathbb{R}_w^{pr}} = \mathbf{v}^T M_{\mathcal{U},h_1 k_1} \mathbf{w}, \quad \text{for } \mathbf{v},\mathbf{w} \in \mathbb{R}^{pr},$$

weighted scalar products and induced norms, indicated by the subscript w. With respect to the weighted norms the coordinate isomorphisms

$$\kappa_{\mathcal{U},h_1 k_1} : \mathcal{U}_{h_1 k_1} \to \mathbb{R}_w^{pr}, u \mapsto \mathbf{u} \quad \text{and} \quad \kappa_{\mathcal{Y},h_2 k_2} : \mathcal{Y}_{h_2 k_2} \to \mathbb{R}_w^{qs}, y \mapsto \mathbf{y}$$

are unitary mappings, since for $u \in \mathcal{U}_{h_1 k_1}$ and $y \in \mathcal{Y}_{h_2 k_2}$ one has

$$\|u\|_{\mathcal{U}} = \|\mathbf{u}\|_{\mathbb{R}_w^{pr}} \quad \text{and} \quad \|y\|_{\mathcal{Y}} = \|\mathbf{y}\|_{\mathbb{R}_w^{qs}}.$$

Thus, the formulation of $\mathbb{G}_S$ via the respective coefficient vectors is given by

$$\mathbf{G} = \mathbf{G}(h_1,k_1,h_2,k_2) = \kappa_{\mathcal{Y}} \mathscr{P}_{\mathcal{Y}} \mathbb{G} \mathscr{P}_{\mathcal{U}} \kappa_{\mathcal{U}}^{-1} : \mathbb{R}^{pr} \to \mathbb{R}^{qs}.$$

Here we have partially omitted the dependencies on the discretization parameters h_1, k_1, h_2, k_2. In the case of a linear I/O map an explicit matrix representation can be obtained via the real valued elements of $\mathbf{H} := M_{\mathcal{Y}} \mathbf{G}$:

$$\mathbf{H}_{ij}^{kl} = [M_{\mathcal{Y}} \kappa_{\mathcal{Y}} \mathscr{P}_{\mathcal{Y}} \mathbb{G}(\mu_l,\phi_j)]_i^k = (\nu_k \psi_i, \mathbb{G}(\mu_l,\phi_j))_{\mathcal{Y}},$$

which is a block-structured matrix in $\mathbb{R}^{qs \times pr}$ with $q \times p$ blocks $\mathbf{H}^{kl} \in \mathbb{R}^{s \times r}$.

The corresponding operator norm of $\mathbb{G}$,

$$\|\mathbb{G}\|_{\mathscr{L}(\mathcal{U},\mathcal{Y})} = \sup_{u \in \mathcal{U}} \frac{\|\mathbb{G}u\|_{\mathcal{Y}}}{\|u\|_{\mathcal{U}}},$$

is then given by

$$\|\mathbf{G}(h_1 k_1, h_2 k_2)\|_{qs \times pr;w} = \sup_{\mathbf{u} \in \mathbb{R}^{pr}} \frac{\|\mathbf{G}\mathbf{u}\|_{\mathbb{R}_w^{qs}}}{\|\mathbf{u}\|_{\mathbb{R}_w^{pr}}}.$$

The following lemma shows that $\mathbf{G}$ approaches $\mathbb{G}$ with a successive refinement of the discretization, using a component-wise inequality of the discretization parameters $(h_1', k_1', h_2', k_2') \leq (h_1, k_1, h_2, k_2)$. [[43, p. 44]] For all $(h_1', k_1', h_2', k_2') > 0$, one has

$$\|\mathbf{G}(h_1, k_1, h_2, k_2)\|_{qs \times pr;w} = \|\mathbb{G}_S(h_1, k_1, h_2, k_2)\|_{\mathscr{L}(\mathcal{U},\mathcal{Y})} \leq \|\mathbb{G}\|_{\mathscr{L}(\mathcal{U},\mathcal{Y})}.$$

If the subspaces $\{\mathcal{U}_{h_1 k_1}\}$ and $\{\mathcal{Y}_{h_2 k_2}\}$ are nested in the sense that

$$\mathcal{U}_{h_1',k_1'} \subset \mathcal{U}_{h_1 k_1}, \quad \mathcal{Y}_{h_2',k_2'} \subset \mathcal{Y}_{h_2 k_2} \quad \text{for } (h_1',k_1',h_2',k_2') \leq (h_1,k_1,h_2,k_2),$$

then $\|\mathbf{G}(h_1, k_1, h_2, k_2)\|_{qs \times pr;w}$ monotonically increases for decreasing discretization parameters $(h_1 k_1, h_2 k_2) > 0$, and $\|\mathbf{G}(h_1 k_1, h_2 k_2)\|_{qs \times pr;w}$ is convergent for $(h_1, k_1, h_2, k_2) \searrow 0$.

4 I/O Maps for Semi-discretized Linearized Navier-Stokes Equations

In this section systems of LNSE as in (2c) are considered, that are already discretized in space, as described for example in [19]. Interpreting them as a system of linear differential-algebraic equations (DAE) of the form (4) with constant coefficients, one can make use of the explicit solution formulas as derived in [13] to obtain a state-space representation of the I/O map.

4.1 An explicit solution formula for DAEs

To describe the explicit solution formula, it is convenient to recall some facts about linear DAEs with constant coefficients. The style and the notation is consistent with [35]. Consider a linear DAE initial value problem

$$\mathcal{E}\dot{x} + \mathcal{A}x = f(t) \quad \text{for } t \in [0,T], \tag{6}$$

$$x(0) = x_0, \tag{7}$$

defined by a matrix pair $(\mathcal{E}, \mathcal{A})$, with $\mathcal{E}, \mathcal{A} \in \mathbb{R}^{n \times n}$ and with a typically singular matrix $\mathcal{E}$. Such a matrix pair $(\mathcal{E}, \mathcal{A})$ with $\mathcal{E}, \mathcal{A} \in \mathbb{R}^{n \times n}$ is called *regular*, if $\det(\lambda \mathcal{E} + \mathcal{A})$ does not vanish identically for all $\lambda \in \mathbb{C}$.

For a regular matrix pair the analysis can be based on the Weierstraß canonical form, see e.g. [17], since if $(\mathcal{E}, \mathcal{A})$ is a regular matrix pair, then there exist nonsingular matrices P_1, P_2 of appropriate dimensions such that

$$(P_1 \mathcal{E} P_2, P_1 \mathcal{A} P_2) = \left(\begin{bmatrix} I_d & 0 \\ 0 & N \end{bmatrix}, \begin{bmatrix} J & 0 \\ 0 & I_a \end{bmatrix} \right),$$

where J is a matrix in real Jordan canonical form and N is a nilpotent matrix also in Jordan canonical form. The index of nilpotency μ of N is called the *differentiation-index* of the corresponding DAE and denoted as $\operatorname{ind}(\mathcal{E}, \mathcal{A}) := \nu$.

If $\mathcal{A}$ is invertible, then one has $\operatorname{ind}(\mathcal{E}, \mathcal{A}) = \operatorname{ind}(\mathcal{E}, I) =: \operatorname{ind}(\mathcal{E})$ and that $\nu = \operatorname{ind}(\mathcal{E})$ is the smallest integer for which $\operatorname{rank} \mathcal{E}^{\nu+1} = \operatorname{rank} \mathcal{E}^{\nu}$ holds. In this case the differentiation index is the matrix index of $\mathcal{E}$.

To obtain the solution formula one needs the *Drazin inverse*, see [10], which for a matrix $\mathcal{E} \in \mathbb{R}^{n \times n}$ with $\operatorname{ind}(\mathcal{E}) = k$ is the unique matrix $X \in \mathbb{R}^{n \times n}$ satisfying

$$
\begin{aligned}
&\text{(D1)} \quad \mathcal{E}X = X\mathcal{E}, \\
&\text{(D2)} \quad X\mathcal{E}X = X, \\
&\text{(D3)} \quad X\mathcal{E}^{k+1} = \mathcal{E}^k.
\end{aligned}
\tag{8}
$$

The solution formula for (4) then is well-known [9, 35]. Let $\mathcal{E}, \mathcal{A} \in \mathbb{R}^{n \times n}$ be a regular matrix pair of commuting matrices. Furthermore, let $f \in C^{\nu}(0, T; \mathbb{R}^n)$ with $\nu = \operatorname{ind}(\mathcal{E}, \mathcal{A})$. Then every solution $x \in C^1(0, T; \mathbb{R}^n)$ of $\mathcal{E}\dot{x} + \mathcal{A}x = f(t)$ has the form

$$x(t) = e^{-\mathcal{E}^D \mathcal{A} t} \mathcal{E}^D \mathcal{E} q + \int_0^t e^{-\mathcal{E}^D \mathcal{A}(t-s)} \mathcal{E}^D f(s) ds +$$

$$(I - \mathcal{E}^D \mathcal{E}) \sum_{i=0}^{\nu-1} (-\mathcal{E} \mathcal{A}^D)^i \mathcal{A}^D f^{(i)}(t) \tag{9}$$

for some $q \in \mathbb{C}^n$.

For the initial value problem (6) the above theorem implies that if q exists such, that

$$x_0 = \mathcal{E}^D \mathcal{E} q + (I - \mathcal{E}^D \mathcal{E}) \sum_{i=0}^{\nu-1} (-\mathcal{E} \mathcal{A}^D)^i \mathcal{A}^D f^{(i)}(0) \tag{10}$$

then there exists a unique solution, provided that $(\mathcal{E}, \mathcal{A})$ form a regular pair of commuting matrices and f is sufficiently smooth.

The commutativity requirement is no restriction for regular matrix pairs, since for a $\hat{\lambda} \in \mathbb{C}$ chosen such that $R(\hat{\lambda}) := (\hat{\lambda} \mathcal{E} + \mathcal{A})$ is invertible, the matrices

$$\hat{\mathcal{E}} := R(\hat{\lambda})^{-1} \mathcal{E} \quad \text{and} \quad \hat{\mathcal{A}} := R(\hat{\lambda})^{-1} \mathcal{A}$$

commute. Since the solvability properties of a DAE system are not affected by a simple scaling from the left, the above results hold for general linear DAEs with a regular pair of coefficient matrices. To apply the solution formula directly for a general system, the matrices $\mathcal{E}, \mathcal{A}$ and the inhomogeneity have to be substituted by

$$\mathcal{E} \leftarrow (\hat{\lambda} \mathcal{E} + \mathcal{A})^{-1} \mathcal{E}, \quad \mathcal{A} \leftarrow (\hat{\lambda} \mathcal{E} + \mathcal{A})^{-1} \mathcal{A} \quad \text{and} \quad f \leftarrow (\hat{\lambda} \mathcal{E} + \mathcal{A})^{-1} f,$$

while the variable vector x remains unchanged.

4.2 Explicit Solution of a Semi-discretized LNSE System

In [13] it has been shown how to specialize the general solution formula (9) using the typical structure of the spatial discretization of the linearized Navier-Stokes equations, which is given by

$$\begin{bmatrix} M & 0 \\ 0 & 0 \end{bmatrix} \frac{d}{dt} \begin{bmatrix} v(t) \\ p(t) \end{bmatrix} + \begin{bmatrix} D & -J^T \\ J & Q \end{bmatrix} \begin{bmatrix} v(t) \\ p(t) \end{bmatrix} = \begin{bmatrix} f_1(t) \\ f_2(t) \end{bmatrix}, \quad \text{for } t \in (0, T], \tag{11}$$

$$v(0) = v_0 \in \mathbb{R}^{n_v}.$$

The functions v and p describe finite dimensional coefficient vectors representing the discretized velocity and pressure field of the flow and are assumed to take on values in $\mathbb{R}^{n_v}$ and $\mathbb{R}^{n_p}$, respectively. The coefficient matrices $M, D \in \mathbb{R}^{n_v, n_v}$, $J \in \mathbb{R}^{n_p, n_v}$ and $Q \in \mathbb{R}^{n_p, n_p}$ are constant. The inhomogeneities in the momentum and continuity equations are given by $f_1(t) \in \mathbb{R}^{n_v}$ and $f_2(t) \in \mathbb{R}^{n_p}$, respectively.

To make the coefficients matrix pair commute, one can scale by $\mathcal{A}^{-1} := \begin{bmatrix} D & -J^T \\ J & Q \end{bmatrix}^{-1}$. The invertibility of $\mathcal{A}$ is a reasonable assumption if the associated stationary problem possesses a unique solution. If we assume further that D is invertible, which is related to the uniqueness of the steady state solution [25] and given for example for the Stokes linearization, then one can use the Schur complement $S := Q + JD^{-1}J^T$ and obtains a system with $\hat{\mathcal{A}} = I$ and

$$\hat{\mathcal{E}} = \begin{bmatrix} E_{11} & 0 \\ E_{21} & 0 \end{bmatrix} := \begin{bmatrix} (I - D^{-1}J^T S^{-1} J) D^{-1} M & 0 \\ -S^{-1} J D^{-1} M & 0 \end{bmatrix}, \tag{12}$$

The state vector $\begin{bmatrix} v \\ p \end{bmatrix}$ is not affected while the inhomogenity (using $R_0 := D^{-1} J^T S^{-1}$) can be expressed as

$$\begin{bmatrix} \hat{f}_1 \\ \hat{f}_2 \end{bmatrix} = \begin{bmatrix} (I - D^{-1}J^T S^{-1} J) D^{-1} f_1 + R_0 f_2 \\ -S^{-1} J D^{-1} f_1 + S^{-1} f_2 \end{bmatrix} = \begin{bmatrix} E_{11} M^{-1} f_1 + R_0 f_2 \\ E_{21} M^{-1} f_1 + S^{-1} f_2 \end{bmatrix}. \tag{13}$$

The explicit solution formula then depends on the index of the pair of coefficients in (11) which is usually $\nu = 2$ and thus the explicit solution formula for (9) is

$$x(t) = e^{-\hat{\mathcal{E}}^D t}\hat{\mathcal{E}}^D \hat{\mathcal{E}} q + \int_0^t e^{-\hat{\mathcal{E}}^D(t-s)}\hat{\mathcal{E}}^D \hat{f}(s)ds - (I - \hat{\mathcal{E}}^D \hat{\mathcal{E}})\sum_{i=0}^{1}(\hat{\mathcal{E}})^i \hat{f}^{(i)}(t)$$

and still requires the computation of the Drazin inverse and the matrix exponential.

It has been shown in [13], that $\operatorname{ind} E_{11} \in \{1, 2\}$ and that the solution of the semi-discretized LNSE (11) equation on $[0, T]$ is given by

$$\begin{bmatrix} v(t) \\ p(t) \end{bmatrix} = \begin{bmatrix} \exp(-E_{11}^D t)E_{11}^D E_{11} q_v \\ E_{21}\exp(-E_{11}^D t)(E_{11}^D)^2 E_{11} q_v \end{bmatrix} + \int_0^t \begin{bmatrix} \exp(-E_{11}^D(t-s))E_{11}^D \hat{f}_1(s) \\ E_{21}\exp(-E_{11}^D(t-s))(E_{11}^D)^2 \hat{f}_1(s) \end{bmatrix} \mathrm{d}s +$$
$$+ \begin{bmatrix} [I - E_{11}^D E_{11}]\hat{f}_1(t) \\ -E_{21}E_{11}^D \hat{f}_1(t) + \hat{f}_2(t) \end{bmatrix} + \begin{bmatrix} [E_{11} - E_{11}^D E_{11}^2]\hat{f}_1^{(1)}(t) \\ [E_{21} - E_{21}E_{11}^D E_{11}]\hat{f}_1^{(1)}(t) \end{bmatrix}, \tag{14}$$

assuming that the vector q_v belongs to a given consistent initial value v_0, c.f. (10).

Furthermore, the last summand can be expressed as

$$\begin{bmatrix} [E_{11} - E_{11}^D E_{11}^2]\hat{f}_1^{(1)} \\ [E_{21} - E_{21}E_{11}^D E_{11}]\hat{f}_1^{(1)} \end{bmatrix} = \begin{bmatrix} [E_{11}^2 - E_{11}^D E_{11}^3]M^{-1}\dot{f}_1 + [E_{11} - E_{11}^D E_{11}^2]R_0\dot{f}_2 \\ [E_{21}E_{11} - E_{21}E_{11}^D E_{11}^2]M^{-1}\dot{f}_1 + [E_{21} - E_{21}E_{11}^D E_{11}]R_0\dot{f}_2 \end{bmatrix}. \tag{15}$$

These results lead to the following results on the dependence of the solution on the (regularity of the) input function. Consider the DAE formulation of the semi-discretized LNSE system (11). If $\mathcal{A}$ and D are invertible and if k is the index of the matrix E_{11} in (12) then the following assertions hold:

1. if $k = 1$, then $\dot{f}_1$ does not appear in the solution and $\dot{f}_2$ appears only in the second component corresponding to the pressure, and

2. if $k = 2$, then $\dot{f}_1$ only appears in the pressure solution.

If the inhomogeneity contains an input functions of low regularity, then to avoid impulses in the solution it would be necessary that $\operatorname{ind}(E_{11}) = 1$. Lemma 10 in [13] gives a sufficient condition for that if D is symmetric. For LNSE with nonsymmetric D one has the following lemma: Consider the LNSE given in (11) and assume that M is positive definite, D is invertible and Q is symmetric and semi-definite, $[J\ Q]$ is of full row rank and $\operatorname{im} J = \ker Q$. Then $\operatorname{ind} E_{11} = 1$, where $E_{11} := (I - D^{-1}J^T S^{-1}J)D^{-1}M$ and $S := Q + JD^{-1}J^T$.

Proof. The symmetry and semi-definiteness of Q imply the existence of an orthogonal matrix $\mathcal{V} \in \mathbb{R}^{n_p \times n_p}$ such that $Q = \mathcal{V}\begin{bmatrix} \Sigma_k & 0 \\ 0 & 0 \end{bmatrix}\mathcal{V}^T$. Here, k is the rank of Q and Σ_k is a diagonal matrix of the nonzero eigenvalues. According to this partition of Q we can write $\mathcal{V} = [V\ W]$, where V spans the image and W spans the kernel of Q, respectively. Since $\operatorname{im} J = \ker Q$, there exists a $X \in \mathbb{R}^{n_p - k \times n_v}$ with full rank and $J = WX$. Defining $S_X := XD^{-1}X^T$ the Schur complement S and its inverse can be written as

$$S = Q + JD^{-1}J^T = [V\ W]\begin{bmatrix} \Sigma_k & 0 \\ 0 & S_X \end{bmatrix}\begin{bmatrix} V^T \\ W^T \end{bmatrix} \quad \text{and} \quad S^{-1} = \begin{bmatrix} V^T \\ W^T \end{bmatrix}\begin{bmatrix} \Sigma_k & 0 \\ 0 & S_X^{-1} \end{bmatrix}[V\ W],$$

8

respectively. With this, we can rewrite E_{11} as

$$E_{11} = (I - D^{-1}X^T W^T \begin{bmatrix} V^T \\ W^T \end{bmatrix} \begin{bmatrix} \Sigma_k & 0 \\ 0 & S_X^{-1} \end{bmatrix} [V \ W] XW) D^{-1} M = (I - D^{-1}X^T S_X^{-1} X) D^{-1} M.$$

Since X has full rank, there exists an orthogonal matrix $U \in \mathbb{R}^{n_v \times n_v}$, such that $X = \begin{bmatrix} G & 0 \end{bmatrix} U$ with G invertible. Then define $\tilde{D} := UD^{-1}U^T$ and $\tilde{M} := UMU^T$ and the block decomposition according to X^T:

$$\tilde{D} = \begin{bmatrix} \tilde{D}_{11} & \tilde{D}_{12} \\ \tilde{D}_{21} & \tilde{D}_{22} \end{bmatrix} \quad \text{and} \quad \tilde{M} = \begin{bmatrix} \tilde{M}_{11} & \tilde{M}_{12} \\ \tilde{M}_{21} & \tilde{M}_{22} \end{bmatrix}.$$

With this, the inverse of S_X is given by

$$(XD^{-1}X^T)^{-1} = (\begin{bmatrix} G & 0 \end{bmatrix} \tilde{D} \begin{bmatrix} G^T \\ 0 \end{bmatrix})^{-1} = G^{-T} \tilde{D}_{11}^{-1} G^{-1},$$

and one can compute E_{11} via

$$(I - D^{-1}X^T S_X^{-1} X) D^{-1} M = (D^{-1} - D^{-1} U^T \begin{bmatrix} G^T \\ 0 \end{bmatrix} G^{-T} \tilde{D}_{11}^{-1} G^{-1} \begin{bmatrix} G & 0 \end{bmatrix} U D^{-1}) M$$

$$= U^T U (D^{-1} - D^{-1} U^T \begin{bmatrix} \tilde{D}_{11}^{-1} & 0 \\ 0 & 0 \end{bmatrix} U D^{-1}) U^T U M$$

$$= U^T (\begin{bmatrix} \tilde{D}_{11} & \tilde{D}_{12} \\ \tilde{D}_{21} & \tilde{D}_{22} \end{bmatrix} - \begin{bmatrix} \tilde{D}_{11} & \tilde{D}_{12} \\ \tilde{D}_{21} & \tilde{D}_{22} \end{bmatrix} \begin{bmatrix} \tilde{D}_{11}^{-1} & 0 \\ 0 & 0 \end{bmatrix} \begin{bmatrix} \tilde{D}_{11} & \tilde{D}_{12} \\ \tilde{D}_{21} & \tilde{D}_{22} \end{bmatrix}) U M$$

$$= U^T (\begin{bmatrix} 0 & 0 \\ 0 & S_{\tilde{D}} \end{bmatrix}) U M,$$

with $S_{\tilde{D}} := \tilde{D}_{22} - \tilde{D}_{21} \tilde{D}_{11}^{-1} \tilde{D}_{12}$ invertible, since $\tilde{D}_{11}$ and $\tilde{D}$ are invertible. Thus, one obtains that E_{11} is similar to the matrix

$$\tilde{E}_{11} = \begin{bmatrix} 0 & 0 \\ 0 & S_{\tilde{D}} \end{bmatrix} U M U^T = \begin{bmatrix} 0 & 0 \\ S_{\tilde{D}} \tilde{M}_{21} & S_{\tilde{D}} \tilde{M}_{22} \end{bmatrix},$$

which is of index 1, since $\tilde{M}_{22}$ as a submatrix of a positive definite matrix is invertible and therefore rank $\tilde{E}_{11}^2 = $ rank $\tilde{E}_{11}$. $\qquad\square$

Lemma 4.2 includes the case of stable finite element schemes where J has full rank and $Q = 0$, c.f. [19], and unstable schemes with a minimal stabilization, c.f. [12].

4.3 Explicit Representation of the I/O Map for LNSE

We can directly imply the formulas in the control context by setting

$$f_1(t) \leftarrow f_1(t) + B_1 u(t) \quad \text{and} \quad f_2(t) \leftarrow f_2(t) + B u_2(t),$$

where B_1, B_2 denote bounded operators that map the control into the source terms. For the output the operator C is applied to the solution. Hence, the system of constraints in the optimal control problem has the form

$$\begin{bmatrix} M & 0 \\ 0 & 0 \end{bmatrix} \frac{d}{dt} \begin{bmatrix} v(t) \\ p(t) \end{bmatrix} + \begin{bmatrix} D & -J^T \\ J & Q \end{bmatrix} \begin{bmatrix} v(t) \\ p(t) \end{bmatrix} = \begin{bmatrix} f_1(t) + B_1 u(t) \\ f_2(t) + B_2 u(t) \end{bmatrix}, \tag{16}$$

$$y(t) = C \begin{bmatrix} v(t) \\ p(t) \end{bmatrix} \quad \text{for } t \in (0, T]. \tag{17}$$

We will consider only the case $B_2 = 0$, since a perturbation of the continuity equation would necessitate a change of the underlying model from incompressible to compressible flow as treated, e.g., in [14]. Following the arguments of Section 4.2 one obtains a representation of an I/O map for (16) via the affine linear map

$y(t) =$

$$
\begin{aligned}
&C \left\{ \begin{bmatrix} \exp(-E_{11}^D t) E_{11}^D E_{11} q_v \\ E_{21} \exp(-E_{11}^D t)(E_{11}^D)^2 E_{11} q_v \end{bmatrix} + \int_0^t \begin{bmatrix} \exp(-E_{11}^D(t-s)) E_{11}^D \hat{f}_1(s) \\ E_{21} \exp(-E_{11}^D(t-s))(E_{11}^D)^2 \hat{f}_1(s) \end{bmatrix} \mathrm{d}s \right. \\
&\quad + \begin{bmatrix} [E_{11} - E_{11}^D E_{11}^2][M^{-1} f_1(t) + [I - E_{11} E_{11}^D] R_0 f_2(t)] \\ E_{21}[I - E_{11}^D E_{11}] M^{-1} f_1(t) + [S^{-1} - E_{21} E_{11}^D R_0] f_2(t)] \end{bmatrix} \\
&\quad + \left. \begin{bmatrix} [E_{11} - E_{11}^D E_{11}^2] R_0 \dot{f}_2(t) \\ E_{21}[E_{11} - E_{11}^D E_{11}^2] M^{-1} \dot{f}_1(t) + [E_{21} - E_{21} E_{11}^D E_{11}] R_0 \dot{f}_2(t) \end{bmatrix} \right\} \quad := y_0
\end{aligned}
$$

$$
\begin{aligned}
&+ C \left\{ \int_0^t \begin{bmatrix} \exp(-E_{11}^D(t-s)) E_{11}^D E_{11} M^{-1} B_1 u(s) \\ E_{21} \exp(-E_{11}^D(t-s))(E_{11}^D)^2 E_{11} M^{-1} B_1 u(s) \end{bmatrix} \mathrm{d}s + \right. \\
&\quad + \left. \begin{bmatrix} [E_{11} - E_{11}^D E_{11}^2] M^{-1} B_1 u(t) \\ E_{21}[I - E_{11}^D E_{11}] M^{-1} B_1 u(t) \end{bmatrix} + \begin{bmatrix} 0 \\ E_{21}[E_{11} - E_{11}^D E_{11}^2] M^{-1} (B_1 u)^{(1)}(t) \end{bmatrix} \right\} \quad := Gu(t).
\end{aligned}
$$
(18)

The linear I/O map is defined via $G : \mathcal{U} \to \mathcal{Y}$, $u \mapsto Gu$, by subtracting the vector y_0.

To obtain a well-defined I/O map, one needs $B_1 u(0)$ to be consistent with the initial condition v_0, c.f. (10), and the function $B_1 u : [0, T] \to \mathbb{R}^{n_v}$ has to be sufficiently smooth. Since B_1 as a bounded operator maintains regularity, one can infer from (18) and Proposition 4.2 the regularity requirements

1. $\mathcal{U} \subset \mathcal{C}^1([0, T], U)$ in the case that $\mathrm{ind}\, E_{11} = 2$ or

2. $\mathcal{U} \subset \mathcal{C}([0, T], U)$ if $\mathrm{ind}\, E_{11} = 1$ or if only the velocity is considered for the output .

In both cases the output space $\mathcal{Y}$ is a subspace of $\mathcal{C}([0, T], Y)$.

In the next section, we use the explicit solution formula to construct error bounds.

5   Error Analysis for the I/O Map

The overall error in the computation of a discretized I/O map consists of the signal approximation error ϵ_S and the dynamical approximation error ϵ_D. The signal approximation error arises from the approximation of $\mathbb{G}$ by $\mathbb{G}_S$ in finite dimensional signal spaces. The dynamical approximation error arises from the actual realization $\mathbb{G}_{DS}$ of the map that takes into account the numerical approximation of the system dynamics. In a suitable operator norm this decomposition is formally obtained via the estimate

$$
\|\mathbb{G}_{DS} - \mathbb{G}\| \leq \|\mathbb{G}_S - \mathbb{G}\| + \|\mathbb{G}_{DS} - \mathbb{G}_S\| =: \epsilon_S + \epsilon_D.
$$
(19)

Since we have assumed that the system is already spatially discretized, only the time integration error is addressed in this section. However, the framework of I/O maps is also well suited for the derivation of goal oriented error estimates and application of corresponding mesh refinement techniques, as discussed in [2, 43].

The error estimates in the following subsections are valid for a concrete spatially discretized LNSE control system and use a notation in line with the previous chapters. An overview is given in Table 1.

∞-dim. system	disc. I/O spaces	time disc. system
$\mathbb{G} : \mathcal{U} \to \mathcal{Y}$	$\mathbb{G}_S : \mathcal{U}_{h_1 k_1} \to \mathcal{Y}_{h_2 k_2}$	$\mathbb{G}_{DS} : \mathcal{U}_{h_1 k_1} \to \mathcal{Y}_{h_2 k_2}$
$G : \mathcal{U} \to \mathcal{Y}$	$G_{h_1 h_2 k_1 k_2} : \mathcal{U}_{h_1 k_1} \to \mathcal{Y}_{h_2 k_2}$	$G_{D;h_1 h_2 k_1 k_2} : \mathcal{U} \to \mathcal{Y}$
	or $G_{\kappa_1 \kappa_2} : \mathcal{U}_{\kappa_1} \to \mathcal{Y}_{\kappa_2}$	$\mathbf{G}, \mathbf{H} : \mathbb{R}^{pr} \to \mathbb{R}^{qs}$

Table 1: Discretized I/O maps. The first line contains the operators for a general system, the second line lists the respective realizations for the LNSE, the simplified subscript notation and their matrix representations.

5.1 Signal Approximation Error

The investigation of the error ϵ_S caused by discretization of the input and output signals uses the framework and the notation introduced in Section 3. We first recall the main elements and introduce some simplifying notations.

The signals $u \in \mathcal{U}$ and $y \in \mathcal{Y}$ are approximated by means of finite dimensional subspaces $\mathcal{U}_{h_1 k_1}$ and $\mathcal{Y}_{h_2 k_2}$ and corresponding orthogonal projectors $\mathscr{P}_{\mathcal{U}, h_1 k_1}$ and $\mathscr{P}_{\mathcal{Y}, h_2 k_2}$. To simplify the notation we introduce the abbreviations $\kappa_1 := h_1 k_1$ and $\kappa_2 := h_2 k_2$. Then, for signals $u \in \mathcal{U}$ and $y \in \mathcal{Y}$, the corresponding approximations are given by

$$u_{\kappa_1} := \mathscr{P}_{\mathcal{U}, \kappa_1} u \quad \text{and} \quad y_{\kappa_2} := \mathscr{P}_{\mathcal{Y}, \kappa_2} y.$$

Combining the projectors with the I/O map G, we obtain the formal approximations as described in Table 1. We have

$$G_{\kappa_2} := \mathscr{P}_{\mathcal{Y}, \kappa_2} G \quad \text{and} \quad G_{\kappa_1 \kappa_2} := \mathscr{P}_{\mathcal{Y}, \kappa_2} G \mathscr{P}_{\mathcal{U}, \kappa_1}.$$

Using this notation, the signal approximation error ϵ_S, describing the deviation in the observation between the actual G and the discretized I/O map $G_{\kappa_1 \kappa_2}$ for an $u \in \mathcal{U}$ in the $\mathcal{Y}$-norm is given by

$$\|G_{\kappa_1 \kappa_2} u - Gu\|_{\mathcal{Y}}^2 = \int_0^T \|G_{\kappa_1 \kappa_2} u(t) - Gu(t)\|_Y^2 \mathrm{d}t.$$

In the following estimates the explicit dependency on t is dropped for convenience. Inserting $G_{\kappa_1} u$ and defining

$$e_{u, \kappa_1} := u - \mathscr{P}_{\mathcal{U}, \kappa_1} u \quad \text{and} \quad e_{y, \kappa_2} := \mathscr{P}_{\mathcal{Y}, \kappa_2} G u_{\kappa_1} - G u_{\kappa_1},$$

the approximation error can be expressed by means of the interpolation errors:

$$\|G_{\kappa_1 \kappa_2} u - Gu\|_{\mathcal{Y}} = \|G_{\kappa_1 \kappa_2} u - G_{\kappa_1} u + G_{\kappa_1} u - Gu\|_{\mathcal{Y}} \leq \|e_{y, \kappa_2}\|_{\mathcal{Y}} + \|G e_{u, \kappa_1}\|_{\mathcal{Y}}.$$

The interpolation errors e_{y, κ_2} and e_{u, κ_1} are estimated with respect to the concrete discretization scheme, as e.g. finite elements in space and wavelets in time.

The explicit representation of the operator G then is helpful to get a better estimate of the transferred input error than $\|Ge_{u,\kappa_1}\|_{\mathcal{Y}} \le \|G\|\|e_{u,\kappa_1}\|_{\mathcal{U}}$, with a possibly rough approximation of $\|G\|$.

Consider for example the case that the output is extracted only from the velocity solution via an output operator C_v. According to the definition of the I/O map, one then obtains G as defined in (18) with $C = \begin{bmatrix} C_v & 0 \end{bmatrix}$. Using the simplifying notation

$$\mathscr{E}_1(\tau) := e^{-\tau E_{11}^D} E_{11}^D M^{-1} \quad \text{and} \quad \mathscr{E}_2 := [E_{11} - E_{11}^D E_{11}^2]M^{-1},$$

a general estimate for the term $\|Ge_{u,\kappa_1}\|_Y^2$ delivers

$$\|G_h e_{u,\kappa_1}\|_Y^2 = \|C_v \Big\{ \int_0^t \mathscr{E}_1(t-s)Be_{u,\kappa_1}\mathrm{d}s + \mathscr{E}_2 Be_{u,\kappa_1} \Big\}\|_Y^2$$

$$\le \|C_v\|_*^2 \, \|\int_0^t \mathscr{E}_1(t-s)Be_{u,\kappa_1}\mathrm{d}s + \mathscr{E}_2 Be_{u,\kappa_1}\|_{\mathbb{R}^{n_v}}^2,$$

with $\|\cdot\|_*$ denoting an operator or matrix norm.

The properties of the scalar product and the Cauchy-Schwarz inequality then lead to the terms $\|\int_0^t \mathscr{E}_1(t-s)\bar{e}_{u,\kappa_1}\mathrm{d}s\|_{\mathbb{R}^{n_v}}$ and $\|\mathscr{E}_2 Be_{u,\kappa_1}\|_{\mathbb{R}^{n_v}}$. The latter can be estimated by

$$\|\mathscr{E}_2 \bar{e}_{u,\kappa_1}\|_{\mathbb{R}^{n_v};w} \le \|E_{11} - E_{11}^D E_{11}^2\|_* \|M^{-1}Be_{u,\kappa_1}\|_{\mathbb{R}^{n_v}},$$

while the first term requires some further treatment.

$$\begin{aligned}
\|\int_0^t \mathscr{E}_1(t-s)Be_{u,\kappa_1}\mathrm{d}s\|_{\mathbb{R}^{n_v}} &= \|\int_0^t e^{-(t-s)E_{11}^D} E_{11}^D M^{-1}Be_{u,\kappa_1}\mathrm{d}s\|_{\mathbb{R}^{n_v}} \\
&\le \int_0^t \|e^{-(t-s)E_{11}^D} E_{11}^D\|_* \|M^{-1}Be_{u,\kappa_1}\|_{\mathbb{R}^{n_v}}\,\mathrm{d}s \\
&\le \left(\int_0^t e^{(t-s)\|E_{11}^D\|_*} \|E_{11}^D\|_* \mathrm{d}s \right) \left(\sup_{s\in[0,t]} \|M^{-1}Be_{u,\kappa_1}\|_{\mathbb{R}^{n_v}} \right) \\
&= \left(e^{t\|E_{11}^D\|_*} - 1 \right) \sup_{s\in[0,t]} \|M^{-1}Be_{u,\kappa_1}\|_{\mathbb{R}^{n_v}}.
\end{aligned}$$

Collecting all the above estimates we obtain the following error estimate. Consider the I/O map (18) defined by the semidiscretized LNSE (16) with $C = [C_v\ 0]$. Let e_{u,κ_1} and e_{y,κ_2} be the interpolation errors in the input and output space for time $t \in [0,T]$, respectively. Then, the following assertions hold.

1. The error in the observation caused by the signal discretization satisfies

$$\|G_{\kappa_1\kappa_2}u - Gu\|_{\mathcal{Y}} \le \|e_{y,\kappa_2}\|_{\mathcal{Y}} + \|Ge_{u,\kappa_1}\|_{\mathcal{Y}}.$$

2. For the response of the input approximation error one has

$$\|Ge_{u,\kappa_1}\|_{\mathcal{Y}} \le \mathrm{c}\sqrt{T}\|C_v\|_* \sup_{t\in[0,T]} \|M^{-1}Be_{u,\kappa_1}\|_{\mathbb{R}^{n_v}},$$

with a constant

$$\mathrm{c} = \left(e^{T\|E_{11}^D\|_*} - 1 + \|E_{11} - E_{11}^D E_{11}^2\|_* \right).$$

5.2 Time Discretization Error

The time integration error, caused by the numerical integration of the spatially discretized state equations, is not of primary interest for the investigation of the I/O behavior. Nevertheless, to ensure meaningful and reliable numerical results, it should be kept small or at least well balanced with respect to the signal approximation error.

Instead of using the explicit solution formula, in the practical treatment the underlying DAE is solved via a numerical integration scheme. Since the spatially discretized system is a DAE of differentiation index 2, one has to use suitable time integration algorithms. For the time discretization of flow problems the literature provides a vast amount of well understood and investigated schemes as well as only partly proven, but "working" approaches. Most of them more or less explicitly carry out an *index reduction* of the DAE system, c.f. [48]. After index reduction, in the present case of a semi-explicit system, there exist several *Runge-Kutta* methods and *backward difference* schemes that are suitable to integrate the equations directly. These methods and proofs of their convergence order can be found in [26].

As an example, for s-stage *Runge-Kutta* methods of type *Radau IIa* the global error is of order τ^{2s-1} in the velocity and of τ^s in the pressure component, where τ denotes the time step size. These orders of convergence, however, are only guaranteed for sufficiently smooth solutions, which require additional regularity of the inhomogeneity, c.f. Section 4.3.

6 Numerical Tests

To demonstrate the described approximation scheme, we have implemented a model problem of a driven cavity flow with Reynolds number 1333 in a two-dimensional square domain, subject to a distributed control and observations that are extracted from the velocity field. The behavior of the fluid is modeled by the LNSE, spatially discretized by stabilized $Q_1 - P_0$ finite elements, which are piecewise linear for the velocity and piecewise constant for the pressure, on a uniform 128×128 grid. The resulting, still time dependent linear DAE system is integrated numerically using a *projection* method as introduced in [18].

All numerical tests are carried out in MATLAB [46]. The open source toolbox IFISS [44] is used as the basis for several routines especially for the spatial discretization and the visualization of the flow field.

6.1 Distributed Control of the Driven Cavity

In order to control the flow in the driven cavity, an input term is added to the spatially discretized LNSE. Also an output has to be defined, along with suitable domains and function spaces. Let $\Omega = (-1, 1)^2$ be the domain of the driven cavity, let $\Omega_c := (-0.2, 0.2) \times (-0.7, -0.5)$ denote the subdomain where the control is active, and let $\Omega_m = (-0.1, 0.1) \times (0, 0.6)$ denote the subdomain where the velocity field is observed, c.f. Figure 1.

With $Y = L_2([0,1])^2$ and $U = L_2([0,1])^2$, we define $C \in \mathscr{L}(L_2(\Omega)^2, Y)$ and $B_1 \in \mathscr{L}(U, L_2(\Omega)^2)$ by

$$(CV)(\xi) = \int_{-0.1}^{0.1} \frac{V(x_1, \theta_m \xi)}{0.2} \, dx_1, \quad (B_1 u)(x_1, x_2) = \begin{cases} u(\theta_c x_1), & (x_1, x_2) \in \Omega_c, \\ 0, & \text{elsewhere,} \end{cases} \quad (20)$$

where $\theta_m : [0, 1] \to [0, 0.6]$ and $\theta_c : [-0.2, 0.2] \to [0, 1]$ are affine linear mappings, that adjust the spatial extensions of the signal spaces to the respective domains Ω_c and Ω_m. By
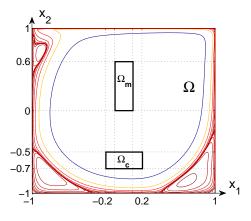
Figure 2: Schematic illustration of a 2D driven cavity flow and the domains of control and observation, Ω_c and Ω_m, respectively.

definition, B_1 maps the two input signal components into the control domain such that they are homogeneous in x_2-direction. The output is extracted as the average in x_1-direction of the velocity within the observation domain and V denotes the weak velocity solution of the underlying ∞-dimensional system.

$$V_t + (V_\infty \cdot \nabla)V + (V \cdot \nabla)V_\infty + \nabla P - \frac{1}{Re}\triangle V = (V_\infty \cdot \nabla)V_\infty + B_1 u,$$
$$\nabla \cdot V = 0,$$
$$y = CV,$$

with initial and boundary conditions $V|_{t=0} = V_\infty$ and $V|_{\partial\Omega} = g$.

Here, g denotes the boundary conditions for the driven cavity which are homogeneous Dirichlet conditions on the whole boundary except at the upper lid, where a constant velocity is applied. The reference velocity and initial condition V_∞ is chosen as the corresponding stationary solution.

6.2   Discretization of the Signal Spaces

In the abstract framework, the discretizations are parameterized by characteristic length scales k_1, k_2, h_1, h_2 that tend to zero with a refinement of the discretization. However, in this concrete setup it is more convenient to call on parameters $H_1, H_2, K_1, K_2 \in \mathbb{N}$ that correspond directly to the dimensions of the signal approximation spaces. In the current case we have that the characteristic length scales are related to the dimension parameters via

$$k_1 = \frac{1}{2^{K_1}}, \quad k_2 = \frac{1}{2^{K_2}}, \quad h_1 = \frac{1}{2^{H_1}+1} \quad \text{and} \quad h_2 = \frac{1}{2^{H_2}+1}. \tag{21}$$

The temporal discretization is carried out by approximating the signal components in $L_2(0, 0.1)$ by piecewise constant functions. The finite dimensional interpolation spaces $\mathcal{R}(k_1)$ and $\mathcal{S}(k_2)$ are defined by means of the *Haar-wavelet* basis, i.e.,

$$\mathcal{R}(k_1) = \text{span}\{\varphi_i\}_{i=1}^{2^{K_1}} \quad \text{and} \quad \mathcal{S}(k_2) = \text{span}\{\varphi_j\}_{j=1}^{2^{K_2}}, \quad K_1, K_2 \in \mathbb{N}, \tag{22}$$

14

with φ_l denoting the l-th *Haar-wavelet* basis function in $[0, 0.1]$, illustrated in Figure 2.

This special choice equips the bases of $\mathcal{R}(k_1)$ and $\mathcal{S}(k_2)$ with the useful properties of orthogonal and hierarchical bases. The hierarchy of bases allows to refine or coarsen the signal discretization by simply adding or removing basis functions, to change e.g. the number of degrees of freedom in $\mathcal{R}(k_1)$ from 2^{K_1} to 2^{K_1+1}.

The restriction of the levels of approximation to $\dim \mathcal{R} \in \{2^k, k \in \mathbb{N}\}$ ensures a uniform resolution on the whole time scale.

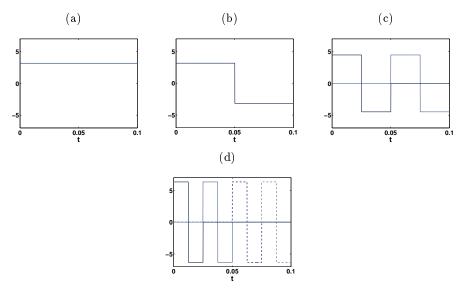(a)   (b)   (c)

(d)

Figure 3: Orthonormal Haar wavelet basis of the $L_2([0, 0.1])$ subspace of piecewise constant functions: (a) φ_1, (b) φ_2, (c) φ_3, φ_4, (d) $\varphi_5, \varphi_6, \varphi_7, \varphi_8$

For the spatial discretization of the spaces $U = Y = [L_2([0, 1])]^2$ a hierarchical basis of piecewise linear functions is chosen. This yields

$$U(h_1) = \operatorname{span}\left\{ \begin{bmatrix} \mu_k \\ 0 \end{bmatrix}, \begin{bmatrix} 0 \\ \mu_k \end{bmatrix} \right\}_{k=1}^{2^{H_1}+1} \quad \text{and} \quad Y(h_2) = \operatorname{span}\left\{ \begin{bmatrix} \mu_l \\ 0 \end{bmatrix}, \begin{bmatrix} 0 \\ \mu_l \end{bmatrix} \right\}_{l=1}^{2^{H_2}+1}$$

for $H_1, H_2 \in \mathbb{N}$ and scalar basis functions μ_i as illustrated in Figure 3. Note that the chosen basis functions do not have local support, such that the corresponding mass matrix is not sparse. However, the possibility to construct a hierarchy of spaces is more important for our purpose.

This approach can easily be extended towards different bases for input and output as well as for the separate components.

In view of the notation in Section 3 the dimensions of the subspaces are abbreviated via

$$\dim U_{h_1} = p(h_1), \quad \dim Y_{h_1} = q(h_1), \quad \dim \mathcal{R}_{k_1} = r(k_1) \quad \text{and} \quad \dim \mathcal{S}_{k_2} = s(k_2).$$

Recalling the identities (21), one obtains the explicit dependencies of H_1, H_2, K_1 and K_2, as for example

$$p(h_1) = 2 \cdot \frac{1}{h_1} = 2 \cdot (2^{H_1} + 1) \quad \text{and} \quad s(k_2) = \frac{1}{k_2} = 2^{K_2}. \tag{23}$$
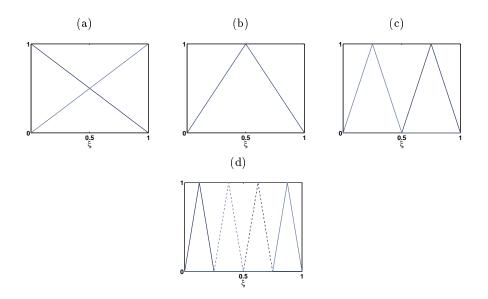
Figure 4: Hierarchical basis of piecewise linear functions of a $L_2([0,1])$ subspace: (a) μ_1, μ_2, (b) μ_3, (c) μ_4, μ_5, (d) $\mu_6, \mu_7, \mu_8, \mu_9$

6.3 Discretized I/O Map for the Driven Cavity

Using the mathematical framework of Section 3, the matrix representation of the I/O map is established by computing the system response for the basis functions in the input space $\mathcal{U}_{h_1 k_1}$ and testing them against all basis functions of the output space $\mathcal{Y}_{h_2 k_2}$. Identifying

$$\text{span}\left\{\begin{bmatrix}\mu_k \\ 0\end{bmatrix}, \begin{bmatrix}0 \\ \mu_k\end{bmatrix}\right\}_{k=1}^{2^{H_1}+1} \quad \text{with} \quad \text{span}\{\eta_l\}_{l=1}^{2\cdot(2^{H_1}+1)},$$

for the input and output space one has

$$\mathcal{U}_{h_1 k_1} = \text{span}\{\eta_k \varphi_i : k = 1, \ldots, p, \ i = 1, \ldots, r\} \tag{24a}$$

and

$$\mathcal{Y}_{h_2 k_2} = \text{span}\{\eta_l \varphi_j : l = 1, k = 1, \ldots, q, \ j = 1, \ldots, s\}, \tag{24b}$$

respectively. With these basis functions one can compute the block-structured matrix

$$\mathbf{H} = \left[H^{kl}\right]_{\substack{k=1,\ldots,p \\ l=1,\ldots,q}}, \quad \text{with} \quad H^{kl} = [(\eta_k \varphi_i, G(\eta_l \varphi_j))_{\mathcal{Y}}]_{\substack{i=1,\ldots,r \\ j=1,\ldots,s}},$$

which maps the input signal coefficient vector $\mathbf{u}_{h_1 k_1} \in \mathbb{R}^{p \cdot r}$ onto $M_{\mathcal{Y}} \mathbf{y}_{h_2 k_2}$, where $M_{\mathcal{Y}}$ denotes the mass matrix corresponding to the discretization of $\mathcal{Y}_{h_2 k_2}$ and where $\mathbf{y}_{h_2 k_2} \in \mathbb{R}^{q \cdot s}$ is the coefficient vector of the discretized system response.

The system response $y = G(u)$ to the input signal is computed by numerical integration of the semi-discretized state equations, i.e., y is a vector containing the function values at discrete points within the time interval. The time integral of the inner product $(y, G_h(\mathbf{u}))_{\mathcal{Y}}$ and the norm $\|y\|_{\mathcal{Y}}$ are approximated using piecewise the trapezoidal rule, which causes an inaccuracy of order 2 with respect to the time step used in the time integration. Recalling that the *projection* algorithms produce a time integration error of first order, c.f. [18], this error may be neglected.

16

6.4 Experimental Analysis of the Convergence in the Signal Approximation

The numerical convergence in the signal approximation is investigated for the test signal $\hat{u}(t; \theta) = [\sin(10\pi t)\sin(10\pi\theta)\ 0]^T$ and its system response $y = G\hat{u}$. The error is expressed via the relative deviation $\|y - \tilde{y}\|_{\mathcal{Y}}\|\hat{u}\|_{\mathcal{U}}$ with $\tilde{y} = G_{h_1 h_2 k_1 k_2}\hat{u}$ for varying discretization parameters H_1, H_2, K_1, K_2, c.f. Equation (21). As predicted by Proposition 4.2 the error behaves like the error for piecewise constant or piecewise linear interpolation, c.f. Figure 4. In particular it decays linearly with a refined time resolution (a) and quadratically if the time discretization is fixed while the spatial resolution is successfully refined (b). However, the space resolution error cannot go beyond the error in the time discretization, as is indicated in the breakdown of the quadratic convergence rate for fine resolutions. Thus, for an effective discretization of the I/O map a proper balance of space and time resolution is indispensable.
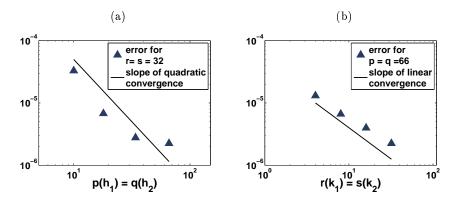

Figure 5: Relative output errors $\|y - \tilde{y}\|_{\mathcal{Y}}\|\hat{u}\|_{\mathcal{U}}$ with $\tilde{y} = G_{h_1 h_2 k_1 k_2}\hat{u}$. Errors for (a) varying $h_1 = h_2$, i.e., varying $\dim \mathcal{U}_{h_1} = \dim \mathcal{Y}_{h_2}$ and fixed $\dim R(k_1) = \dim S(k_2) = 32$ and (b) for varying $k_1 = k_2$ and fixed $\dim \mathcal{U}_{h_1} = \dim \mathcal{Y}_{h_2} = 2 \cdot 33$.

Another property of the system becomes evident in the asymmetry depicted in the Tables 2 and 3. These tables show the evolution of the signal approximation error when the discretization of the input and output signals is changed independently. The imbalance in

$K_1 \backslash K_2$	2	3	4	5
2	**1.00000**	0.55114	0.37103	0.25052
3	0.97709	**0.50776**	0.30652	0.15711
4	0.97619	0.50545	**0.30363**	0.16634
5	0.97626	0.50519	0.30235	**0.17153**

Table 2: Relative errors $e_{K_1, K_2} := \frac{\|y - G_{\hat{h}_1, \hat{h}_2, k_1, k_2}\hat{u}\|_{\mathcal{Y}}}{\|y - G_{\hat{h}_1, \hat{h}_2, k_1=2, k_2=2}\hat{u}\|_{\mathcal{Y}}}$ for a fixed space resolution $\hat{H}_1 = \hat{H}_2 = 5$ and varying K_1 and K_2

Table 2, in the sense that $e_{i,j} > e_{j,i}$ for $i > j$, illustrates the fact that, with respect to the time resolution, it is better to do a refinement in the output space rather than in the input space.

In Table 3 one can observe that a refinement of the space resolution of the signals is more

$H_1 \backslash H_2$	2	3	4	5
2	**1.00000**	0.99878	0.99871	0.99870
3	0.21177	**0.20530**	0.20488	0.20485
4	0.09981	0.08516	**0.08414**	0.08408
5	0.08679	0.06945	0.06819	**0.06811**

Table 3: Relative errors $e^{H_1,H_2} = \frac{\|y - G_{h_1 h_2 \hat{k}_1 \hat{k}_2} \hat{u}\|_{\mathcal{Y}}}{\|y - G_{h_1=2,h_2=2,\hat{k}_1 \hat{k}_2} \hat{u}\|_{\mathcal{Y}}}$ for a fixed space resolution $\hat{K}_1 = \hat{K}_2 = 5$ and varying H_1 and H_2.

effective in the input than in the output space.

7 Application to Optimal Flow Control

We illustrate the use of a discretized I/O map $\mathbf{G}$ for the approximate solution of an optimization problem

$$\mathcal{J}(u, Gu) \to \min, \quad \text{for } u \in \mathcal{U}, \tag{25}$$

with a cost functional $J : \mathcal{U} \times \mathcal{Y} \to \mathbb{R}$ of the form $\mathcal{J}(u, Gu) = \frac{1}{2}\|y_0 + Gu - y_D\|_{\mathcal{Y}}^2 + \alpha\|u\|_{\mathcal{U}}^2$. Here $y_D \in \mathcal{Y}$ is a desired output and $\alpha > 0$ is a regularization parameter that penalizes the energy of the input u. This optimization aims at an input u that causes an output $y_a := y_0 + Gu$ that is close to a target state in the norm of $\mathcal{Y}$, while the control effort $\|u\|_{\mathcal{U}}^2$ is not too large. Recall that the actual output of the system is recovered by adding the affine component y_0 to Gu, c.f. (18).

Following the notation in Section 6 we define the discrete signal spaces $\mathcal{U}_{h_1,k_1}$ and $\mathcal{Y}_{h_2,k_2}$. With the vector representations of the approximations $\mathbf{y}_D := \kappa_{\mathcal{Y},h_2,k_2}\mathscr{P}_{\mathcal{Y},h_2,k_2} y_D$ and $\mathbf{y}_0 := \kappa_{\mathcal{Y},h_2,k_2}\mathscr{P}_{\mathcal{Y},h_2,k_2} y_0$ we define the discrete cost functional

$$\bar{\mathcal{J}} : \mathbb{R}^{pr} \times \mathbb{R}^{qs} \to \mathbb{R}, \qquad \bar{\mathcal{J}}(\mathbf{u}, \mathbf{Gu}) = \frac{1}{2}\|\mathbf{Gu} + \mathbf{y}_0 - \mathbf{y}_D\|_{\mathbb{R}_w^{qs}}^2 + \alpha\|\mathbf{u}\|_{\mathbb{R}_w^{pr}}^2. \tag{26}$$

Then a solution of (25) can be approximated by the solution $\bar{\mathbf{u}} = \text{argmin}\{\bar{\mathcal{J}}(\mathbf{u}, \mathbf{Gu}) : \mathbf{u} \in \mathbb{R}^{qs}\}$ given by

$$(\mathbf{G}^T \mathbf{M}_{\mathcal{Y}} \mathbf{G} + \alpha \mathbf{M}_{\mathcal{U}})\bar{\mathbf{u}} = \mathbf{G}^T \mathbf{M}_{\mathcal{Y}}(\mathbf{y}_D - \mathbf{y}_0). \tag{27}$$

For the special choice of $H_1 = H_2 = K_1 = K_2 = 4$ the linear system (27) has a system matrix $\mathbf{G}$ of dimension $34 \cdot 16 \times 34 \cdot 16$. Using the standard routines of MATLAB [46], the solution of (27) takes 0.0334 seconds on a standard desktop PC equipped with OpenSuse 11.0 and an Intel dual core processor with 2 GHz.

As an application example we consider the driven cavity as described in Section 6.1 and the task of finding inputs that cause a prescribed output y_D in the domain of observation via the solution of (27). Figure 5 shows the result for $y_D \equiv [1\ 0]^T$. This choice for y_D is supposed to force a flow field in the domain of observation, that is 1 in the x_1 component and zero in the second component, c.f. the construction of the output in (20). Figure 6 illustrates the result for $y_D \equiv [0\ 1]^T$ aiming at a zero x_1 component and a 1 in the x_2 component in the velocity field across the domain of observation.
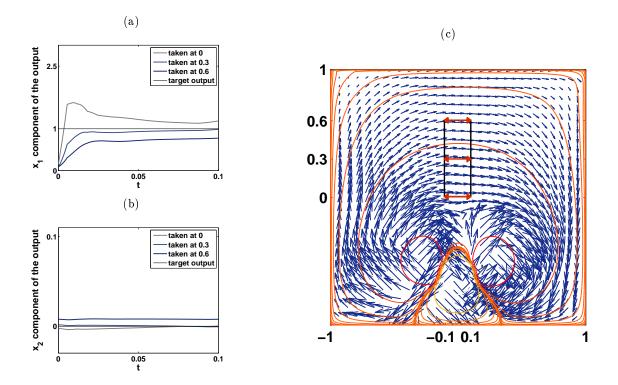
Figure 6: Illustration of the system response for an input $\bar{u}$ that was computed via (27) to match an output $y_D = [1\ 0]^T$. (a) and (b) show the time evolution of the output signal at three distinguished points in the domain of observation. Plot (c) shows the velocities and the stream lines of the corresponding flow field.

8   Summary and Outlook

Using the explicit solution (14) formula for the spatially discretized linearized Navier-Stokes equations (LNSE) we have obtained a closed formula for the relation between the input and the output for a distributed control of LNSE. Error estimates using hierarchical bases of finite dimensional in- and output spaces were derived and conditions for the necessary regularity of the input functions have been established. One observation is that in the general case one can use functions of low regularity like Haar-wavelets and lower order finite elements for the discretization of the input, if only the velocity component is considered. The numerical results back the theoretical error bounds and show the applicability of the chosen approach.

From the theoretical point of view it remains to analyze the regularity conditions for the input with respect to the spatial discretization schemes and how to characterize adequate initial conditions. Another important question is to extend the approach to problems with boundary control and the fully nonlinear Navier-Stokes equations. Furthermore the presented approach has to be checked for efficiency and robustness against other approaches, like empirical *black box* schemes or *model predictive control.*
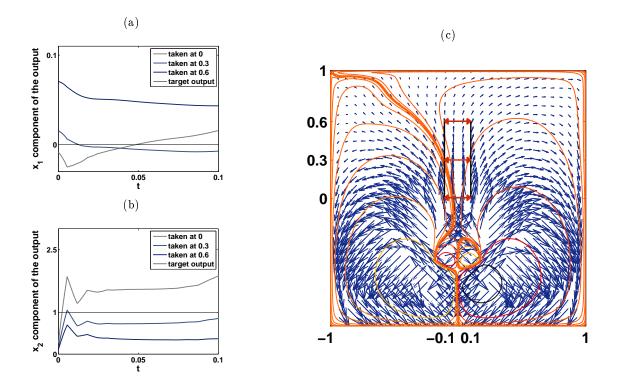
Figure 7: Illustration of the system response for an input $\bar{u}$ that was computed via (27) to match an output $y_D = [0\ 1]^T$. (a) and (b) show the time evolution of the output signal at three distinguished points in the domain of observation. Plot (c) shows the velocities and the stream lines of the corresponding flow field.

References

[1] A. C. Antoulas, Approximation of large-scale dynamical systems (Society for Industrial and Applied Mathematics (SIAM), Philadelphia, 2005).

[2] W. Bangerth and R. Rannacher, Adaptive finite element methods for differential equations (Birkhäuser, Basel, 2003).

[3] R. Becker, M. Garwon, C. Gutknecht, G. Bärwolff, and R. King, Robust control of separated shear flows in simulation and experiment, J. of Process Control **15**, 691–700 (2005).

[4] P. Benner, V. Mehrmann, V. Sima, S. Van Huffel, and A. Varga, SLICOT—a subroutine library in systems and control theory, in: Applied and computational control, signals, and circuits, Vol. 1, , Appl. Comput. Control Signals Circuits, Vol. 1 (Birkhäuser Boston, Boston, MA, 1999), pp. 499–539.

[5] P. Benner, V. Mehrmann, and D. Sorensen (eds.), Dimension Reduction of Large-Scale Systems (Springer, 2005).

[6] A. Bensoussan, G. Da Prato, M. C. Delfour, and S. K. Mitter, Representation and control of infinite dimensional systems. Volume I. (Birkhäuser, Boston, MA, 1992).

[7] G. Berkooz, P. Holmes, and J. L. Lumley, The proper orthogonal decomposition in the analysis of turbulent flows, in: Annual review of fluid mechanics, Vol. 25, (Annual Reviews Inc., Palo Alto, 1993), pp. 539–575.

[8] T. R. Bewley, R. Temam, and M. Ziane, A general framework for robust control in fluid mechanics, Physica D **138**(3-4), 360–392 (2000).

[9] S. L. Campbell, Singular Systems of Differential Equations I (Pitman, San Francisco, CA, 1980).

[10] S. L. Campbell and C. D. Meyer, Generalized Inverses of Linear Transformations (Pitman, San Francisco, CA, 1979).

[11] K. Deckelnick and M. Hinze, Semidiscretization and error estimates for distributed control of the instationary Navier-Stokes equations, Numer. Math. **97**(2), 297–320 (2004).

[12] H. C. Elman, D. J. Silvester, and A. J. Wathen, Finite elements and fast iterative solvers: with applications in incompressible fluid dynamics (Oxford University Press, Oxford, UK, 2005).

[13] E. Emmrich and V. Mehrmann, Analysis of a class of operator differential-algebraic equations arising in fluid mechanics. Part 1. The finite dimensional case, Tech. rep., TU Berlin, 2010.

[14] E. Feireisl, Dynamics of viscous compressible fluids (Oxford University Press, Oxford, UK, 2004).

[15] E. Fernández-Cara, S. Guerrero, O. Y. Imanuvilov, and J. P. Puel, Remarks on exact controllability for Stokes and Navier-Stokes systems, C. R., Math., Acad. Sci. Paris **338**(5), 375–380 (2004).

[16] R. W. Freund, Model reduction methods based on Krylov subspaces, Tech. rep., Bell Laboratories, Lucent Technologies, 2001.

[17] F. R. Gantmacher, The theory of matrices. Vol. 1. Transl. from the Russian by K. A. Hirsch. Reprint of the 1959 translation (AMS Chelsea Publishing, Providence, RI, 1998).

[18] P. M. Gresho and S. T. Chan, On the theory of semi-implicit projection methods for viscous incompressible flow and its implementation via a finite element method that also introduces a nearly consistent mass matrix. II: Implementation, Int. J. Numer. Methods Fluids **11**(5), 621–659 (1990).

[19] P. M. Gresho and R. L. Sani, Incompressible flow and the finite element method. Vol. 2: Isothermal laminar flow (Wiley, Chichester, UK, 2000).

[20] S. Gugercin and A. C. Antoulas, A survey of model reduction by balanced truncation and some new results, Internat. J. Control **77**, 748–766 (2004).

[21] M. D. Gunzburger, Perspectives in flow control and optimization (Society for Industrial and Applied Mathematics (SIAM), Philadelphia, PA, 2003).

[22] M. D. Gunzburger, L. Hou, and T. Svobodny, Analysis and finite element approximation of optimal control problems for the stationary Navier-Stokes equations with distributed and Neumann controls, Math. Comput. **57**(195), 123–151 (1991).

[23] M. D. Gunzburger and S. Manservisi, Analysis and approximation of the velocity tracking problem for Navier-Stokes flows with distributed control., SIAM J. Numer. Anal. **37**(5), 1481–1512 (2000).

[24] M. D. Gunzburger and S. Manservisi, The velocity tracking problem for Navier-Stokes flows with boundary control, SIAM J. Control Optimization **39**(2), 594–634 (2000).

[25] W. Hackbusch, Elliptic differential equations: theory and numerical treatment (Springer, Berlin, Germany, 1992).

[26] E. Hairer, C. Lubich, and M. Roche, The numerical solution of differential-algebraic systems by Runge-Kutta methods (Springer, Berlin, Germany, 1989).

[27] J. Heiland, V. Mehrmann, and M. Schmidt, A new discretization framework for input/output maps and its application to flow control, in: Active Flow Control. Papers contributed to the Conference "Active Flow Control II 2010", Berlin, Germany, May 26 to 28, 2010, edited by R. King (Springer, Berlin, 2010).

[28] M. Heinkenschloss, D. C. Sorensen, and K. Sun, Balanced truncation model reduction for a class of descriptor systems with application to the Oseen equations, SIAM J. Sci. Comput. **30**(2), 1038–1063 (2008).

[29] L. Henning, D. Kuzmin, V. Mehrmann, M. Schmidt, A. Sokolov, and S. Turek, Flow control on the basis of a Featflow-Matlab coupling, in: Active Flow Control. Papers contributed to the Conference "Active Flow Control 2006", Berlin, Germany, September 27 to 29, 2006, edited by R. King (Springer, Berlin, 2006).

[30] M. Hinze, Instantaneous closed loop control of the Navier-Stokes system, SIAM J. Control Optimization **44**(2), 564–583 (2005).

[31] M. Hinze and K. Kunisch, Second order methods for boundary control of the instationary Navier-Stokes system, ZAMM, Z. Angew. Math. Mech. **84**(3), 171–187 (2004).

[32] L. S. Hou and T. P. Svobodny, Optimization problems for the Navier-Stokes equations with regular boundary controls, J. Math. Anal. Appl. **177**(2), 342–367 (1993).

[33] R. King (editor), Active flow control. Papers contributed to the conference 'Active flow control 2006', Berlin, Germany, September 27–29, 2006 (Springer, Berlin, Germany, 2007).

[34] R. King (editor), Active flow control II. Papers contributed to the conference 'Active flow control II 2010', Berlin, Germany, May 26–28, 2010 (Springer, Berlin, Germany, 2010).

[35] P. Kunkel and V. Mehrmann, Differential-algebraic equations. Analysis and numerical solution (European Mathematical Society Publishing House, Zürich, Switzerland, 2006).

[36] J. L. Lions, On the controllability of distributed systems, Proc. Natl. Acad. Sci. USA **94**(10), 4828–4835 (1997).

[37] D. M. Luchtenburg, B. Günter, B. R. Noack, R. King, and G. Tadmor, A generalized mean-field model of the natural and actuated flows around a high-lift configuration, J. Fluid Mech. **623**, 283–316 (2009).

[38] V. Mehrmann and T. Stykel, Balanced truncation model reduction for large-scale systems in descriptor form, in: Dimension Reduction of Large-Scale Systems, edited by P. Benner, V. Mehrmann, and D. Sorensen (Springer, Heidelberg, 2005), pp. 83–115.

[39] B. R. Noack, M. Schlegel, B. Ahlborn, G. Mutschke, M. Morzynski, P. Comte, and G. Tadmor, A finite-time thermodynamics of unsteady fluid flows, J. Non-Equilib. Thermodyn. **33**(2), 103–148 (2008).

[40] M. Pastoor, L. Henning, B. R. Noack, R. King, and G. Tadmor, Feedback shear layer control for bluff body drag reduction, J. Fluid Mech. **608**, 161–196 (2008).

[41] M. Pošta and T. Roubíček, Optimal control of Navier-Stokes equations by Oseen approximation, Comput. Math. Appl. **53**(3-4), 569–581 (2007).

[42] C. W. Rowley, Model reduction for fluids, using balanced proper orthogonal decomposition, Internat. J. Bifur. Chaos Appl. Sci. Engrg. **15**(3), 997–1013 (2005).

[43] M. Schmidt, Systematic Discretization of Input/Output Maps and other Contributions to the Control of Distributed Parameter Systems, PhD thesis, TU Berlin, Fakultät Mathematik und Naturwissenschaften, Berlin, Germany, 2007.

[44] D. J. Silvester, H. C. Elman, and A. Ramage, IFISS software package [http://www.maths.manchester.ac.uk/~djs/ifiss/], University of Manchester, UK, 2006.

[45] T. Stykel, Balanced truncation model reduction for semidiscretized Stokes equation, Linear Algebra Appl. **415**(2-3), 262–289 (2006).

[46] The MathWorks, Inc., Cochituate Place, 24 Prime Park Way, Natick, MA, Matlab, matlab version 7.11.0 (r2010b), 2008.

[47] C. Tischendorf, Coupled systems of differential algebraic and partial differential equations in circuit and device simulation, Habilitationsschrift, HU Berlin, 2003.

[48] J. Weickert, Applications of the theory of differential-algebraic equations to partial differential equations of fluid dynamics, PhD thesis, TU Chemnitz, Fakultät f. Mathematik, Chemnitz, Germany, 1997.